Electronic Supplementary Information (ESI)

Novel recyclable BiOBr/Fe_3O_4/RGO composites with remarkable visible-light photocatalytic activity

Mingkun Zheng,[a] Xinguo Ma,[a,*] Jisong Hu,[a] Xinxin Zhang,[b,*] Di Li,[c] Wangyang Duan [a]

[a] *School of Science and Hubei Collaborative Innovation Center for High-efficiency Utilization of Solar Energy, Hubei University of Technology, Wuhan, 430068, China*

[b] *Key Laboratory of Material Chemistry for Energy Conversion and Storage, Ministry of Education, Hubei Key Laboratory of Material Chemistry and Service Failure, School of Chemistry and Chemical Engineering, Huazhong University of Science and Technology, Wuhan, 430074, China*

[c] *School of Metallurgical Engineering, Xi'an University of Architecture and Technology, Xi'an, 710055, China.*

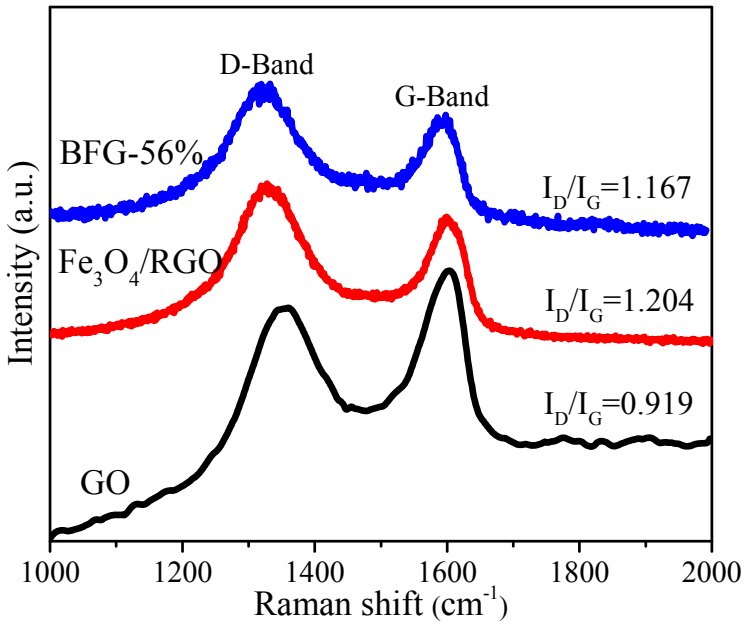

Fig. S1. Raman spectra of GO, Fe_3O_4/RGO and BFG-56%.

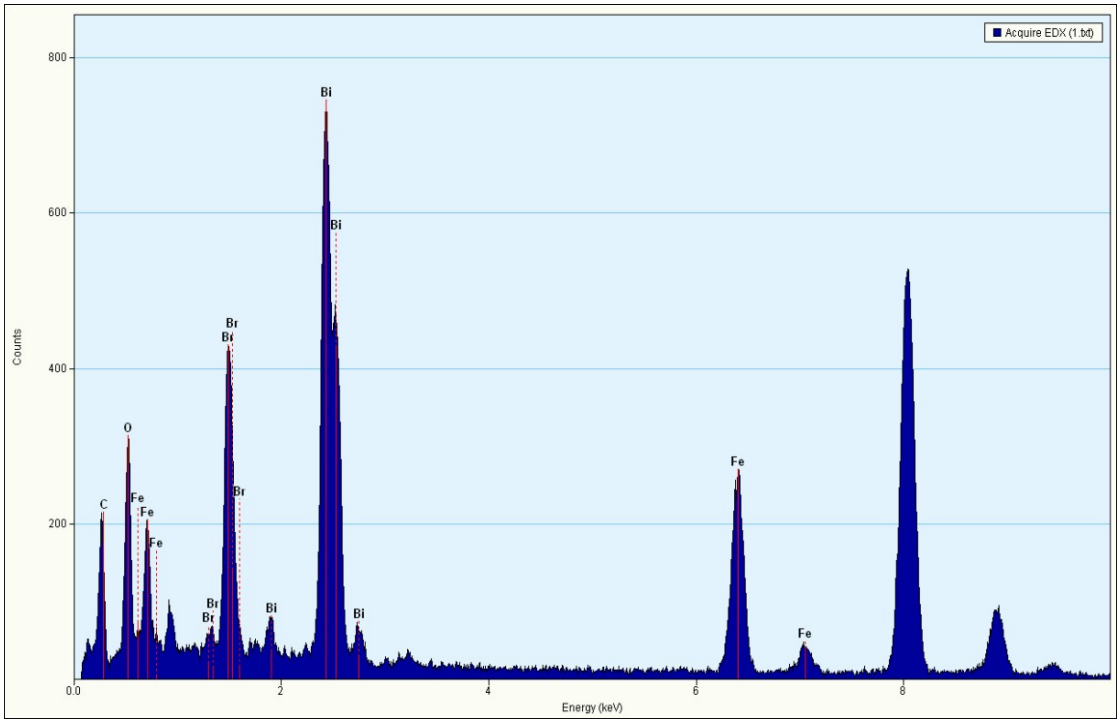

Fig. S2. TEM-EDS spectrum of BFG-56%.

Preparation of BiOBr/RGO

10mg BiOBr was slowly added to 3.2 mL of GO (1mg/mL) suspension，respectively. After vigorously stirring for 4 h, the resulting mixture was poured into a 20 mL Teflon-lined autoclave and heated to 160 °C. for 12 h. The obtained solid precipitate was centrifuged, washed several times with deionized water and absolute ethanol to remove residual ions, and the final product was dried in air at 60 °C to obtain powdery samples. The synthesized composite materials were designated as BiOBr/RGO.

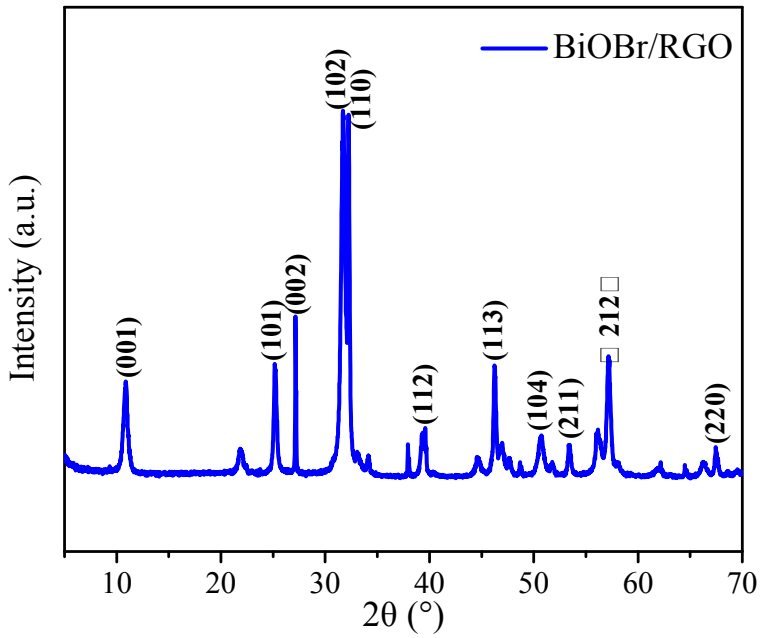

Fig. S3. XRD patterns of BiOBr/RGO.

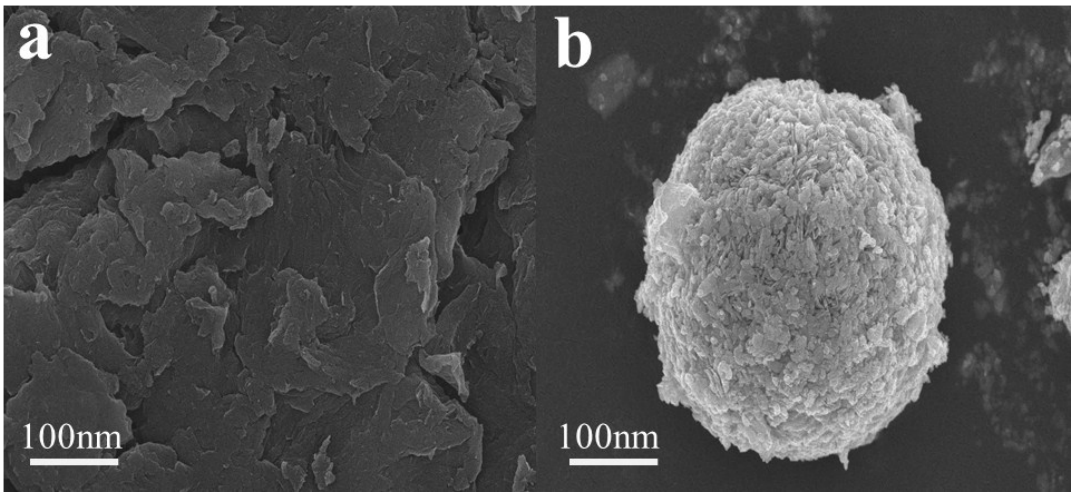

Fig. S4. SEM images of (a) RGO and (b) BiOBr/RGO.

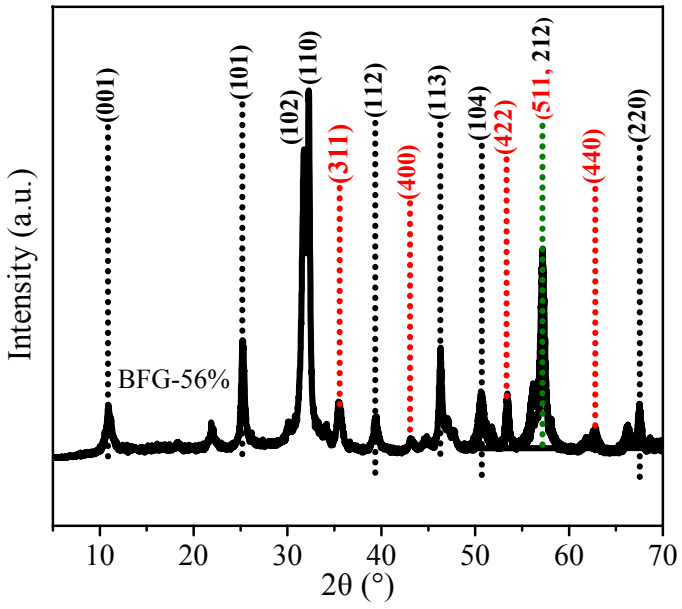

Fig. S5. XRD pattern of BFG-56% after recycling.

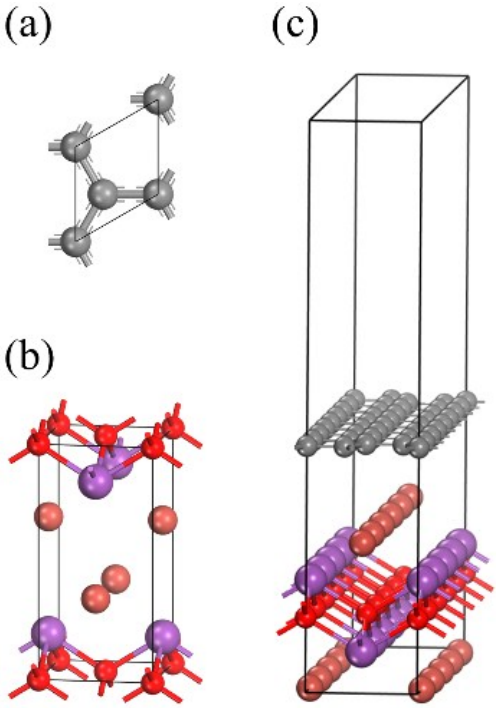

Fig. S6. Optimized geometric structures of (a)RGO, (b) BiOBr, and (c) BiOBr/RGO heterostructure. (gray, red, violet and orange spheres represent C, O, Bi and Br atoms, respectively). For interpretation of the references to color in this figure legend, the reader is referred to the Web version of this article.

In order to model BiOBr/Fe_3O_4/RGO heterostructure, the optimized structures were constructed at first. The {001} facets of BiOBr was normally selected because the {001} facets with 1 layer of Br termination have ignorable cleavage energies, and accordingly, an extremely high thermodynamic stability. Furthermore, the {001} facet was experimentally confirmed as the active crystal plane with high photocatalytic activity. And then, a 5×1 relaxed BiOBr (001) surface, a 8× $\sqrt{3}$ RGO formed heterostructure, as shown in the Fig. S6.

Table S1. The k_{app} values of different photocatalysis degradation of RhB in the literature under visible light irradiation

Photocatalysts	k_{app} (BiOBr) min^{-1}	k_{app} (BiOBr based composites) min^{-1}	Increase multiple	Ref.
GO/BiOBr	0.15	0.049	0.3	[1]
Ag-modified BiOBr	0.020	0.023	0.87	[2]
$LaFeO_3$/BiOBr	0.099	0.1301	1.32	[3]
CdS/BiOBr	0.037	0.050	1.35	[4]
BiOBr/BiOI	0.034	0.056	1.65	[5]
BiOBr/RGO	0.029	0.052	1.79	[6]
BiOBr@TiO_2	0.033	0.061	1.85	[7]
BiOBr/UiO-66-NH_2	0.064	0.119	1.86	[8]
BiOBr-Fe_3O_4/RGO	0.036	0.071	1.97	[9]
MoS_2/BiOBr	0.022	0.055	2.50	[10]
BiOBr/Fe_3O_4/RGO	0.022	0.049	2.23	This work

Table S2. Total Mulliken Atomic Populations of RGO and BiOBr layers before and after contact for BiOBr/RGO heterostructure.

	C	O	Br	Bi
RGO (before)	4.00			
BiOBr (before)		6.90	7.51	3.59
RGO (after)	4.03			
BiOBr (after)		6.90	7.26 (7.52)	3.62
Charge transfer	0.03	0.00	-0.25 (0.01)	0.03

References

[1] S. Vadivel, M. Vanitha, A. Muthukrishnaraj and N. Balasubramanian, Journal of Water Process Engineering, 2014, 1, 17–26.

[2] R. Bibi, Q.H. Shen, L.F. Wei, D. Hao, N.X. Li and J.C. Zhou, RSC advances, 2018, 8, 2048–2058.

[3] L. Lu, L. Kong, Z. Jiang, H.C. Lai, T. Xiao and P.P. Edwards, Catalysis Letter, 2012, 142, 771–778.

[4] W. Cui, W. An, L. Liu, J. S. Hu, Y.H. Liang, Applied Surface Science, 2014, 319, 298-305.

[5] L. Lin, M.H. Huang, L.P. Long, Z. Sun, W. Zheng and D.H. Chen, Ceramics International, 2014, 40, 11493–11501.

[6] X.Z. Ren, Y.H. Sun, X. Hu, K. Wu, W. Wang, J. Yin, S.J. Yao, X.C. Zhao and H. Yang, Journal of Nanoparticle Research, 2019, 21, 1–14.

[7] Y. Zhao, H. Xiang, X. Tan, T. Yu, X.L. Li, L.B. Yang and S.C. Wang, Applied Surface Science, 2016, 365, 209–217.

[8] S. Guan, H. Yang, X.F. Sun and T. Xian, Optical Materials, 2020, 100, 109644–109655.

[9] H.F. Xu, Z. Xu, J. Zhou, G. Yan, X.W. Li and S. Zhuo, Ceramics International, 2019, 45, 15458–15465.

[10] J. Di, J.X. Xia, Y.P. Ge, L. Xu, H. Xu, J. Chen, M. He and H. Li, Dalton Trans, 2015, 44, 10156–10165.